

IMPAIRED STRUCTURAL CONNECTIVITY IN PARKINSON'S DISEASE PATIENTS WITH MILD COGNITIVE IMPAIRMENT: A STUDY BASED ON PROBABILISTIC TRACTOGRAPHY.

Inguanzo A (1,2,3), Segura B * (1,2,3,4), Sala-Llonch R (1,3,5,6), Monte-Rubio G (1,2), Abos A (1,2,3), Campabadal A (1,2,3), Uribe C (1,2,3), Baggio HC (1,2), Marti MJ (1,3,4,7), Valldeoriola F (1,3,4,7), Compta Y (1,3,4,7), Bargallo N(8,9), Junque C (1,2,3,4)

1. Institute of Neurosciences, University of Barcelona. Barcelona, Catalonia, Spain.
2. Medical Psychology Unit, Department of Medicine, University of Barcelona. Barcelona, Catalonia, Spain.
3. Institute of Biomedical Research August Pi i Sunyer (IDIBAPS). Barcelona, Catalonia, Spain.
4. Centro de Investigación Biomédica en Red sobre Enfermedades Neurodegenerativas (CIBERNED: CB06/05/0018-ISCI) Barcelona, Catalonia, Spain.
5. Department of Biomedicine, University of Barcelona. Barcelona, Catalonia, Spain.
6. Centro de Investigación Biomédica en Red en Bioingeniería, Biomateriales y Nanomedicina (CIBER-BBN), Barcelona, Catalonia, Spain.
7. Movement Disorders Unit, Neurology Service, Hospital Clínic de Barcelona. Institut de Neurociències. University of Barcelona. Barcelona, Catalonia, Spain.
8. Centre de Diagnostic per la imatge, Hospital Clínic de Barcelona. Barcelona, Catalonia, Spain.
9. Magnetic Resonance Core Facility. Institute of Biomedical Research August Pi i Sunyer (IDIBAPS). Barcelona, Catalonia, Spain

* Corresponding author. Medical Psychology Unit, Department of Medicine. University of Barcelona, Casanova 143, 08036, Barcelona, Spain.

E-mail addresses: annainguanzo@ub.edu (A. Inguanzo), bsegura@ub.edu (B. Segura), roser.sala@ub.edu (R. Sala-Llonch), gmonte@ub.edu (G. Monte-Rubio), alexandraabos@ub.edu (A. Abos), anna.campabadal@ub.edu (A. Campabadal), carme.uribe@ub.edu (C. Uribe), hbaggio@ub.edu (H.C. Baggio), mjmarti@clinic.cat (M.J.

Marti), fvallde@clinic.cat (F. Valldeoriola), ycompta@clinic.cat (Y. Compta), bargallo@clinic.cat (N. Bargallo), cjunque@ub.edu (C. Junque).

KEYWORDS: Parkinson's disease, mild cognitive impairment, magnetic resonance imaging, DTI, probabilistic tractography, TFNBS.

ABSTRACT

Background. Probabilistic tractography, in combination with graph theory, has been used to reconstruct the structural whole-brain connectome. Threshold-free network-based statistics (TFNBS) is a useful technique to study structural connectivity in neurodegenerative disorders; however, there are no previous studies using TFNBS in Parkinson's disease (PD) with and without mild cognitive impairment (MCI).

Methods. Sixty-two PD patients, 27 of whom classified as PD-MCI, and 51 healthy controls (HC) underwent diffusion-weighted 3T MRI. Probabilistic tractography, using FSL, was used to compute the number of streamlines (NOS) between regions. NOS matrices were used to find group differences with TFNBS, and to calculate global and local measures of network integrity using graph theory. A binomial logistic regression was then used to assess the discrimination between PD with and without MCI using non-overlapping significant tracts. Tract-based spatial statistics (TBSS) were also performed with FSL to study changes in fractional anisotropy (FA) and mean diffusivity (MD).

Results. PD-MCI showed 37 white matter (WM) connections with reduced connectivity strength compared to HC, mainly involving temporo-occipital regions. These were able to differentiate PD-MCI from PD without MCI with an area under the curve of 83-85%. PD without MCI showed disrupted connectivity in 18 connections involving fronto-temporal regions. No significant differences were found in graph measures. Only PD-MCI showed reduced FA compared with HC.

Discussion. TFNBS based on whole-brain probabilistic tractography can detect structural connectivity alterations in PD with and without MCI. Reduced structural connectivity in fronto-striatal and posterior corticocortical connections is associated with PD-MCI.

Impact statement

Our data help to clarify that whole-brain connectome analysis based on probabilistic tractography is a useful and sensitive approach to explore the role of WM damages as a relevant pathological substrate of cognitive deficits in PD. Our results might add some evidence regarding the involvement of mostly posterior cortical regions and their connections in PD patients with worse cognitive prognosis. Therefore, TFNBS approach might indicate that structural connectivity abnormalities are not a global phenomenon, and suggest the implication of regional and predominantly posterior structural network disruption underlying cognitive impairment in PD.

INTRODUCTION

Parkinson's disease (PD) is a neurodegenerative disorder chiefly known for its motor symptoms; however, the course of PD is also accompanied by a broad range of non-motor features, including cognitive decline (Kalia and Lang 2015). Mild cognitive impairment (MCI) is a common trait of PD that may be present in its earliest stages, gradually advancing with the progression of the disease and potentially leading to dementia, thus unfavourably affecting the patient's quality of life (Antonini et al. 2012).

Different neuroimaging approaches have been used to describe neuroanatomical correlates of MCI in PD. Previous studies comparing PD-MCI with healthy controls (HC) and PD without MCI have revealed global gray matter atrophy (Segura et al. 2014) and ventricular enlargement (Dalaker et al. 2010; Segura et al. 2014), as well as cortical thinning mainly involving posterior regions (Pereira et al. 2014; Segura et al. 2014). Nevertheless, little is known about the relevance of white matter (WM) microstructure degeneration in PD, or specifically in PD-MCI. Diffusion-weighted MRI (DWI) is a commonly used acquisition method to study the complex organization of WM tracts. However, tract-based spatial statistics (TBSS), a commonly used analysis method based on whole-brain voxel-based fractional anisotropy (FA) measures, have not been conclusive in characterizing WM alterations in PD, as some have found decreased FA in the corpus callosum (Garcia-Diaz et al. 2018), corona radiata as well as internal and external capsule (Li et al. 2018) when comparing PD with HC, while others did not find significant results (Worker et al. 2014).

In addition, a few studies have focused on PD-MCI, showing decreased FA compared to HC in major associative tracts, the corona radiata and the corpus callosum (Agosta et al. 2014; Hattori et al. 2012; Melzer et al. 2013), but others did not find FA differences between PD-MCI patients and PD without MCI using TBSS (Galantucci et al. 2017).

Tractography is another DWI technique, which permits reconstruction of WM tracts and quantification of the local fiber density. This approach, in combination with graph theory, has been used to identify integration and segregation abnormalities in the reconstructed structural whole-brain connectome of PD patients (Abbasi et al. 2020; Mishra et al. 2020;

Nigro et al. 2016). Galantucci and colleagues studied structural connectivity across different brain systems and found PD-MCI to have reduced structural connectivity in networks including the basal ganglia and frontoparietal regions when compared with HC and with PD patients without MCI. Wang and colleagues found decreased structural connectivity in PD-MCI patients in comparison to PD without MCI in several subnetworks, as well as reduced nodal efficiency, mostly involving orbitofrontal regions (Wang et al. 2019). The two studies mentioned above have used a deterministic tractography approach (Galantucci et al. 2017; Wang et al. 2019). However, with this approach, estimating the true trajectories of WM tracts becomes a relevant problem in the context of crossing or kissing fibers (Mori and Van Zijl 2002). In order to surmount this limitation, and to account for uncertainty in the estimation of the models at each voxel, probabilistic tractography algorithms have been proposed (Behrens et al. 2007). Muller and colleagues used both types of tractography in the same PD sample and demonstrated the benefits of probabilistic tractography over the deterministic one (Muller et al. 2019). Given this, other studies have opted for probabilistic tractography to study PD patients (Abbasi et al. 2020; Barbagallo et al. 2017; Shah et al. 2017). Some of the reported findings are decreased clustering coefficient (Shah et al. 2017), decreased global efficiency and increased path length in PD as well as disrupted networks, which were mainly subcortical and already present in the early stages of the disease (Abbasi et al. 2020). In addition, changes in brain network metrics, such as decreased global efficiency and increased characteristic path length, have been found to correlate with a decline in global cognition (Abbasi et al. 2020).

When aiming to describe specific patterns of connectivity alterations in an edge-wise fashion, network-based statistic (NBS) (Zalesky et al. 2010) has been one of the most frequently used methods. Using NBS, many studies have described reduced connectivity in PD compared with HC (Barbagallo et al. 2017; Gou et al. 2018; Nigro et al. 2016; Shah et al. 2017). In the last years, the development of the threshold-free network-based statistics (TFNBS) method (Baggio et al. 2018) which, unlike NBS, does not require the a priori definition of a component-defining threshold and generates edge-wise significant values, has been proposed as a step forward. TFNBS has been proved to be able to detect alterations in the organization and topology of WM tracts, along with the potential to

correctly distinguish between neurodegenerative motor disorders (Abos et al. 2019a; Abos et al. 2019b).

To the best of our knowledge, there is no previous work studying TFNBS based on probabilistic tractography and graph theory analysis to characterize whole-brain structural connectivity in PD-MCI. In this regard, the present study aims to investigate potential abnormalities associated with mild cognitive impairment in PD in the complex structural brain networks.

METHODS

Participants

The initial sample included 69 PD patients recruited from the Parkinson's Disease and Movement Disorders Unit, Hospital Clínic (Barcelona, Spain), and 54 HC from the Institut d'Envel·liment, Universitat Autònoma de Barcelona. Inclusion criteria for patients were (i) fulfilling UK PD Society Brain Bank diagnostic criteria for PD and (ii) no surgical treatment with deep-brain stimulation. Exclusion criteria for all participants were (i) dementia according to Movement Disorders Society criteria, (ii) Hoehn and Yahr (H&Y) scale score > 3, (iii) severe psychiatric or neurological comorbidity, (iv) low global intelligence quotient estimated by the Vocabulary subtest of the Wechsler Adult Intelligence Scale 3rd edition (scalar score ≤ 7), (v) Mini Mental State Examination (MMSE) score below 25, (vi) claustrophobia, (vii) pathological MRI findings other than mild WM hyperintensities in the FLAIR sequence, and (viii) MRI artifacts. A total of 62 PD patients and 51 HC were finally selected. The following participants were excluded from the study: 5 patients and 2 HC with MRI artifacts, 2 patients with claustrophobia and one HC with a cyst. Motor symptoms were assessed with the Unified Parkinson's Disease Rating Scale, motor section (UPDRS-III).

All PD patients were taking antiparkinsonian drugs that consisted of different combinations of L-dopa, catechol-O-methyltransferase inhibitors, monoamine oxidase inhibitors, dopamine agonists, and amantadine. To standardize the doses, the L-dopa equivalent daily dose (LEDD) (Tomlinson et al. 2010) was calculated. Written informed consent was obtained from all study participants after a full explanation of the procedures.

The study was approved by the institutional Ethics Committee from the University of Barcelona (IRB00003099).

Neuropsychological Tests

All participants underwent a comprehensive neuropsychological assessment in the *on* state addressing cognitive domains frequently impaired in PD (Litvan et al. 2012). Attention and working memory were assessed with the Trail Making Test (parts A and B), Digit Span Forward and Backward, Stroop Color-word Test, Symbol Digits Modalities Test (SDMT)-Oral version. Executive functions were evaluated with phonemic and semantic fluencies. Language was assessed by the Boston Naming Test (BNT). Memory was assessed using Rey's Auditory Verbal Learning Test total learning recall, delayed recall and recognition abilities (RAVLT total, RAVLT recall, and RAVLT recognition, respectively). Visuospatial and visuoperceptual functions were assessed with Benton's Judgement of Line Orientation (JLO), Visual Form Discrimination (VFD), and Facial Recognition (FRT) tests. Neuropsychiatric symptoms were evaluated with the Beck Depression Inventory-II, Starkstein's Apathy Scale and Cumming's Neuropsychiatric Inventory. Expected z scores adjusted for age, sex, and education were calculated for each test and subject based on a multiple regression analysis performed in the HC (Aarsland et al. 2009). The presence of MCI was defined using PD-MCI diagnostic criteria level II (Litvan et al. 2012).

MRI acquisition

MRI data were acquired with a 3 T scanner (MAGNETOM Trio, Siemens, Germany). The scanning protocol included high-resolution 3-dimensional T1-weighted images acquired in the sagittal plane (TR = 2300 ms, TE = 2.98 ms, TI = 900 ms, 240 slices, FOV = 256 mm; 1 mm isotropic voxel), two sets of single band spin echo diffusion weighted images in the axial plane with opposite (anteriorposterior and posterioranterior) phase encoding directions (TR = 7700 ms, TE = 89 ms, FOV = 244 mm; 2 mm isotropic voxel; number of directions = 30, b-value = 1000 s/mm², b₀ value = 0 s/mm²) and a T2-weighted axial FLAIR sequence (TR = 9000 ms, TE = 96 ms).

MRI preprocessing

Structural MRI preprocessing was performed using the automated FreeSurfer (version 5.1; available at: <https://surfer.nmr.mgh.harvard.edu/>) pipeline. The cerebral cortex was parcellated into gyral and sulcal structures based on 68 cortical regions of interest (ROIs) from the Desikan-Killiany atlas (Desikan et al. 2006), and 18 deep grey matter (DGM) ROIs from the automated FreeSurfer segmentation step (Filipek et al. 1994; Fischl and Dale 2000; Seidman et al. 1997). DWI images were preprocessed with the FMRIB Software Library (FSL; version 5.08, available at: <https://fsl.fmrib.ox.ac.uk/fsl>). The preprocessing steps included brain extraction using BET, susceptibility-induced distortion correction using topup, and eddy-current distortion and subject motion correction with eddy. FMRIB's Diffusion Toolbox (FDT) was used for data processing, local diffusion modelling and tractography (Jbabdi et al. 2012).

Tract-based spatial statistics

Preprocessed diffusion MRI images were analyzed with FDT software from FSL, (<http://www.fmrib.ox.ac.uk/fsl>). Individual FA maps were obtained using a Diffusion Tensor Model fit (DTIFIT), and the voxel-wise statistical analysis of FA was carried through with TBSS (Smith et al. 2006). TBSS performs non-linear registration (using FNIRT) of FA images from DTIFIT to the MNI standard space and generates a mean FA skeleton that represents the center of all WM tracts common to the whole group. Each subject's FA image was projected onto the skeleton and the resulting FA skeleton images were fed into a general linear model (GLM) modelling the three groups (HC, PD without MCI, PD-MCI) in order to find vertex-wise differences in FA skeleton maps. The same steps were employed to obtain the MD maps. The global mean FA and mean diffusivity (MD) were also extracted.

Tractography and structural connectivity analysis

In order to run probabilistic tractography, the 86 ROIs previously obtained with FreeSurfer were linearly registered from native structural space to native diffusion space with FLIRT (FMRIB's Linear Image Registration Tool) (Jenkinson et al. 2002) to be used as seeds. Next, Bedpostx was applied to calculate the probability distribution of fiber directions in each

voxel (Behrens et al. 2007). Then, we ran the tractography with the Probrtarckx2 tool (Behrens et al. 2007) using 5000 streamlines from each ROI (<http://www.fmrib.ox.ac.uk/fsl>), and a ROI-by-ROI connectivity setting (<https://fsl.fmrib.ox.ac.uk/fsl/fslwiki/FDT/UserGuide#ROIxROI>) obtaining a 86x86 connectivity matrix per each subject, which contained the number of reconstructed streamlines (NOS) between each pair of ROIs. NOS was taken as a measure of the strength of structural connectivity between these regions. To minimize false-positive connections, streamlines intersecting fewer than two regions were ignored, and those detected in at least 50% of the individuals were considered (Abos et al. 2019b; Zalesky et al. 2010). Finally, to test tract-wise differences between groups in interregional NOS, we used TFNBS (Baggio et al. 2018), which performs statistical inference on the data matrix. Results were corrected using family-wise error rate (FWE) correction, with a significance level of $p < 0.05$. Whole-brain NOS was also calculated as the mean of all NOS values.

Graph theory computation

Graph-theory topological parameters derived from the thresholded NOS matrices were obtained using the Brain Connectivity Toolbox (BCT) from MATLAB. The graph metrics included global and local normalized clustering coefficient, global and local node degree, small worldness, normalized path length, modularity, local efficiency and betweenness centrality (See Rubinov and Sporns 2010 (Rubinov and Sporns 2010) for detailed definitions and calculations of the graph metrics).

Additional statistical analyses

Demographic, neuropsychological, and clinical statistical analyses were conducted using IBM SPSS Statistics 25.0 (IBM Corp., Armonk, New York). To assess differences in demographic, clinical and neuropsychological quantitative variables Kruskal-Wallis or Mann-Whitney U tests were used. The chi-squared test was used for categorical variables. Intergroup comparisons for summary graph measures, as well as for global mean FA; MD and NOS were assessed with GLM using in-house MATLAB scripts and Monte Carlo simulations with 5,000 permutations. Results were corrected for multiple testing using FWE correction, with a significance level of $p < 0.05$. Correlations between

neuropsychological test scores as well as clinic data and global FA measures and NOS were evaluated using Pearson correlation.

Additional analyses were conducted to explore differences between PD with and without MCI. For this purpose, the number of connections with significantly reduced connectivity strength in PD-MCI patients compared to HC was matched to those obtained in PD without MCI compared to HC, and the overlapping connections were excluded. The resulting non-overlapping connections were used to calculate their capacity to discern between both groups of PD patients. This set of connections was split into corticocortical and cortico-DGM. To observe if both sets of connections could separately discriminate between PD with and without MCI, a binomial logistic regression for classification was performed using MATLAB (The MathWorks, Inc.; R2019b). Binomial logistic regression is based on a regression model to predict the probability that, for a given input data, each input belongs to a numeric category (0 or 1). It models data using a sigmoid function and becomes a classification technique when a threshold is established on the sigmoid (0.5). The receiver operating characteristic (ROC) curve was obtained from the probability estimations by the logistic regression as scores, as well as the corresponding area under the curve (AUC).

RESULTS

Demographic and clinical characteristics of PD

PD patients and the HC group did not differ significantly in age or years of education, but they did in gender (Supplementary material 1). Twenty-seven PD patients were classified as PD-MCI, and 35 without MCI. Regarding the sociodemographic and clinical characteristics of the three groups (HC, PD without MCI and PD-MCI), shown in Table 1, no significant differences between groups were observed for age, years of education nor global cognition (MMSE). A significant effect was found in gender ($p=0.006$). PD groups did not differ in disease duration, LEDD nor in motor disease severity as measured by the UPDRS-III scale. There was a difference in H&Y scores ($p=0.044$) between subgroups.

Neuropsychological Differences Between Groups

Table 2 shows differences in neuropsychological performance between groups. PD-MCI patient scores were significantly worse than those of PD without MCI and HC in all tests

except forward and backward digits, and BNT. PD-MCI patients also showed lower scores than HC in VFD and FRT.

Tract-based spatial statistics analysis

The TBSS analysis did not show significant differences between PD and HC in FA nor MD. However, when the PD sample was subdivided according to the presence of MCI, PD-MCI patients showed reduced FA compared to HC ($p = 0.031$) (Figure 1). Concretely, decreased FA was detected in the left inferior fronto-occipital fasciculus, corticospinal tract, inferior and superior longitudinal fasciculus and forceps major. There were no differences between PD without MCI and HC, nor between PD subgroups. In contrast, TBSS analysis on MD maps did not show any significant results.

Comparisons in global mean FA did not show significant differences when either comparing PD and HC ($F = 1.102$; $p = 0.323$) or when comparing PD-MCI or PD without MCI with HC ($F = 1.104$; $p = 0.339$).

No significant intergroup differences in global mean MD were found either between PD patients and HC ($F = 0.126$; $p = 0.723$) or when assessing the three previously mentioned groups ($F = 0.546$; $p = 0.588$).

TFNBS analysis

The PD patient group showed reduced number of streamlines (NOS) compared to HC in 114 connections (FWE-corrected, $p < 0.05$). From these 114 connections, 67 were found to be corticocortical (59%), 46 were cortico-DGM (40%) and only one was a DGM-DGM connection (1%). No connections showed significantly higher NOS in PD patients compared with HC. Figure 2 shows the violin plots distribution of the average NOS derived from the 114 connections.

When studying the two PD groups separately, we found that both PD-MCI and PD without MCI showed reduced NOS compared to HC; specifically, patients with PD-MCI showed a higher number of altered connections than PD without MCI (Figure 3). However, differences between PD-MCI and PD without MCI did not reach statistical significance. PD-MCI showed reduced connectivity in 37 connections when compared with HC, 16 of which were corticocortical (43%), mainly involving temporal and occipital regions, and 21 were cortico-DGM (57%). At the same time, PD without MCI showed reduced structural

connectivity compared to HC in 18 connections mainly involving frontal and temporal regions. Twelve connections were corticocortical (67%), 5 were cortico-DGM (28%) and only 1 was a DGM-DGM connection (5%). No connections showed significantly higher NOS in any of the PD groups compared with HC (Supplementary material 2).

Whole-brain mean NOS was significantly reduced in PD compared to HC ($T = 2.78$, $p = 0.003$). When divided into PD-MCI and PD without MCI, both subgroups showed decreased whole-brain mean NOS compared to HC ($T = 2.56$, $p = 0.008$ for PD-MCI and $T = 2.13$, $p = 0.022$ for PD without MCI; FWE-corrected).

We then selected the connections that were differentially altered in PD-MCI and did not overlap with the ones altered in PD without MCI, and we evaluated their discriminatory capabilities using classification metrics. The ROC analysis showed that corticocortical connections with reduced NOS in PD-MCI compared to HC determined a good AUC of 0.83 in distinguishing patients with MCI from those without MCI. In the same line, for DGM-cortical connections we obtained an AUC of 0.85 (Supplementary material 3 and 4).

NOS and FA values did not correlate with clinical variables nor with cognitive performance.

Graph analysis

No group effect was found for global graph parameters, which included the normalized clustering coefficient, mean node degree, small worldness, normalized path length and modularity (Table 3). However, we found differences in local graph measures (FWE-corrected, $p < 0.05$), which implied decreased local efficiency, node degree and nodal clustering coefficient in both PD groups compared to HC (Table 4). Of note, we found differences between PD groups according to MCI presence. PD without MCI had higher nodal clustering coefficient in the left banks of the superior temporal sulcus, postcentral, transverse temporal cortices, as well as in the right superior parietal cortex in comparison to PD-MCI (Table 4). PD-MCI patients, on the other hand, showed higher local efficiency and nodal clustering coefficient in the right accumbens, as well as increased node degree in the left banks of the superior temporal sulcus, when compared to PD without MCI.

DISCUSSION

We have studied structural connectivity alterations in PD and PD-MCI by assessing local changes in WM integrity with TBSS, pair-wise connectivity measures using TFNBS, and global as well as local measures of network integrity using graph theory. As far as we know, this is the first work investigating structural connectivity using TFNBS based on probabilistic tractography in PD-MCI.

PD patients showed a reduced NOS compared to HC. Structural connectivity reduction was present in both PD-MCI and PD without MCI patients. Specifically, PD-MCI showed a higher number of abnormal connections involving cortico-DGM connections and mainly posterior corticocortical regions. PD patients without MCI, in turn, showed fewer impaired connections, mostly located in bilateral prefrontal regions. Our data suggest that whole-brain connectome analysis based on probabilistic tractography is a useful and sensitive approach to explore the structural abnormalities related to cognitive decline in PD.

Whole-brain analysis of pair-wise connections showed reduced NOS in PD compared to HC in 114 connections. Particularly, PD-MCI showed reduced connectivity in a higher number of connections than PD without MCI, which were mainly fronto-striatal and posterior corticocortical connections. A previous study identified decreased global FA and increased global MD as well as structural brain connectivity changes in certain subnetworks based on FA and MD values, which included basal ganglia as well as frontal and parietal nodes in PD-MCI patients in comparison to HC (Galantucci et al. 2017). Similarly, our results showed reduced NOS in fronto-striatal connections, which are known to be related to early cognitive deficits in PD including those commonly described as dopaminergic fronto-striatal executive impairments (Schapira, Chaudhuri, and Jenner 2017). In agreement with our results, Galantucci and colleagues did not find differences in global NOS between PD patient subgroups; nonetheless, both PD-MCI and PD without MCI groups showed reduced global NOS in comparison to HC (Galantucci et al. 2017). In addition, in their study, initial FA NBS analyses showed no differences between PD patients. However, when more liberal statistical thresholds were used, FA connection changes were identified, and were similar to PD changes between controls and PD-MCI patients. In contrast with the results of Galantucci et al., that found decreased FA in PD-MCI compared to HC in a

bilateral principal connected component, we identified significant differences mainly in the left hemisphere. The differences could be due to the sample characteristics, as Galantucci et al. performed the analysis using matched PD samples. However, our results agree with those of Agosta et al, (2014), that reported decreased FA in PD-MCI compared with HC in several left tracts. A recent review of DTI in PD and other parkinsonism showed that, although FA decreases are often bilateral, there are also different studies showing only left hemisphere decreases (Zhang et al. 2020, review). The origin of hemispheric asymmetries is unknown; however, the unilateral findings do not necessarily imply that the other hemisphere is not affected, the non-significant results may be a consequence of the specific threshold established for statistical significance.

In our study, moreover, PD-MCI patients showed reduced NOS in corticocortical connections mainly including temporal and occipital regions. In this context, posterior cortical-based neuropsychological deficits have been related to a higher risk of evolution to dementia (Williams-Gray et al. 2007). This hypothesis is supported by findings from other modalities: FDG-PET data has shown that posterior cortical hypometabolism may play an important role in the pathogenesis of cognitive impairment in PD (Garcia-Garcia et al. 2012; Wu et al. 2018). Moreover, regional cortical thinning in parietotemporal regions, as well as increased global atrophy, have been suggested as structural neuroimaging markers of cognitive impairment in nondemented PD patients (Segura et al. 2014; Uribe et al. 2016). Furthermore, based on pathological findings, the presence of cortical Lewy body pathology, as well as concomitant Alzheimer pathology, seem to be the most relevant factor in the development of cognitive impairment in PD (Halliday et al. 2014). A possible explanation is that neuronal cell bodies could be affected, with gradual loss of synaptic terminals, but dendritic arborization and neuronal connections could also be affected'. Therefore, WM abnormalities observed in cognitively impaired patients may be understood as secondary to axonal degeneration after neuronal body damage. Within this framework, our results might add some evidence regarding the involvement of mostly posterior cortical regions and their connections in PD patients to worse cognitive prognosis.

In our work, logistic regression and ROC curve analysis showed that decreased corticocortical and cortico-DGM connections described in the group comparison between PD-MCI patients and HC can identify subgroups of patients with an AUC of 83% and 85% respectively. Although our analyses were done in order to provide a quantification of the results obtained from the whole connectome, they are in accordance with results from recent approaches that have assessed the discriminant value of features extracted from MRI modalities. A previous study showed that structural connectivity data are relevant in distinguishing parkinsonian patients at the single-subject level with an overall accuracy of 82.23% (Abos et al. 2019b). In PD patients, this MRI data is also able to correctly discern PD patients from HC in longitudinal studies, obtaining similar accuracy results (83.6%) (Peña-Nogales et al. 2019). Only one previous study in PD-MCI (Galantucci et al. 2017) showed that structural abnormalities identified throughout the NBS approach could discriminate PD-MCI from those with PD without MCI with an 81% accuracy.

On the other hand, in our study, other measures derived from DTI showed lower sensitivity to WM abnormalities. We did not find significant differences between groups using mean global measures such as mean global FA and MD. Moreover, only PD-MCI patients compared to HC showed microstructural damage measured by TBSS. Previous literature using this methodological approach suggested that WM damage was emerging as a relevant pathological substrate of cognitive deficits in PD patients (Baggio et al. 2018; Hattori et al. 2012). While some studies identified widespread bilateral WM abnormalities in PD-MCI compared to PD without cognitive impairment in the left corticospinal tract, inferior longitudinal fasciculus and forceps major (Agosta et al. 2014), others found more spatially restricted regions limited to the corona radiata (Melzer et al. 2013), and the posterior part of the corpus callosum (Garcia-Diaz et al. 2018) or did not find significant differences (Galantucci et al. 2017; Hattori et al. 2012).

Characterizing the structural connectome through graph theory provides information about the organization of the network (Griffa et al. 2013). Few studies have investigated the WM structural network connectome alterations in PD-MCI patients. In our study, graph analysis of global network properties did not show significant differences. Similarly, although Wang et al. 2019 reported decreased global efficiency and increased shortest

path length in PD-MCI compared to HC, both important indicators of network interconnectivity, they did not find significant differences between PD subgroups or PD without MCI and HC (Wang et al. 2019). Contrarily, Galantucci et al. (2017), using FA and MD matrices, found increased assortativity – i.e., the preference of a node to connect with similar nodes – and reduced clustering coefficient and global efficiency when comparing PD with and without MCI, suggesting global abnormalities in structural networks (Galantucci et al. 2017). Moreover, our exploratory analysis brought noteworthy differences in local graph measures to light. PD patients showed less local efficiency, nodal degree and clustering coefficient in several regions. Intergroup comparisons mostly suggested decreased in nodal clustering coefficient, specifically in the left banks of the superior temporal sulcus, postcentral, transverse temporal cortices, as well as in the right superior parietal cortex in PD-MCI, in comparison to PD patients without cognitive impairment. The opposite trend was observed only in the right accumbens together with increased node degree in the left banks of the superior temporal sulcus. Widespread regions with decreased nodal efficiency have been previously observed between PD subgroups and HC. However, when PD-MCI and PD without MCI were compared, the reported regions only involved the left olfactory cortex and the left superior frontal gyrus, but not posterior regions (Wang et al. 2019). In this sense, it should be pointed out that the reproducibility of network metrics can be affected by many factors. One relevant aspect would be that previous studies estimated structural connectivity using deterministic tractography, whereas our results were based on a probabilistic approach. Methodological differences as well as diversity in patient characteristics could be contributing to the heterogeneity of these results. Previous results, taken altogether, highlighted the involvement of complex structural brain networks in PD-related cognitive impairment, rather than degeneration of individual WM tracts. Nevertheless, our TFNBS analysis, which allowed us to find a predominant reduction of NOS between PD patients and HC with no a priori selection of tracts, as well as the graph analysis results, might indicate that these structural abnormalities are not a global phenomenon and suggest the implication of regional and predominantly posterior structural network disruption underlying cognitive impairment in PD.

By combining the different methods, we aimed to surpass their individual limitations and give a more accurate vision of structural connectivity in PD-MCI. TBSS is a method that can detect changes in FA throughout the WM of the brain simultaneously. At the same time, although it is a user-friendly method that delivers comprehensive images, it may also cover relevant aspects of the data, as it only makes use of the FA map and discards the orientations' information, leading to complications when it comes to anatomical specificity in regions where paths of different structures merge (Bach et al. 2014). On the other hand, DTI fiber tracking measurements are derived from individual WM connections, and they do allow us to distinguish between adjacent connections, while they may also introduce spurious WM connections that do not exist, limitation that we had tried to minimize by ignoring streamlines intersecting fewer than two regions, and only considering the connections between pairs of regions that were detected in at least 50% of the individuals; while other approaches to the method, such as constrained spherical deconvolution, had managed to improve it (Jeurissen et al 2011). Additionally, graph theory facilitates study of the topological properties of an entire network, instead of the individual analysis of large numbers of tracts, but it has its limitations as well, as these parameters are influenced by the number of nodes of the network, which are indeed arbitrarily chosen. For this reason, we selected well-implemented and standardized atlases.

As expected, in line with previous studies (Segura et al. 2014), our neuropsychological results showed significantly worse performance in verbal memory, semantic fluency, visuospatial and visuo-perceptive functions and processing speed in PD-MCI compared to PD without MCI and HC. However, although altered WM has been recurrently associated with PD-MCI, we did not find significant correlations between cognition and WM measures in accordance with previous studies (Agosta et al. 2014). Although there are several authors that found significant correlations between neuropsychological performance and FA decreases (Zhang et al. 2020, review), they usually combine PD with and without MCI. Greater variability in the degree of cognitive impairment as well as in FA reductions favors the finding of correlations. It is probable that, in our sample, there is not enough variability within the PD-MCI group to provide statistical significance. Regarding the studies using NBS only one reported significant correlations between the neuropsychological

performance and graph measures, but they did not distinguish between PD with and without MCI (Wang et al 2019).

On the other hand, it could also be considered that cognitive impairment is mainly explained by GM degeneration. For example, when both GM and WM changes are considered in the same sample, WM appears to be explaining just a small part of the degenerative pattern. In Inguanzo et al (2021), we used GM and WM measures to perform a hierarchical cluster analysis, and we found 3 subgroups, of which only one presented WM alterations. Accordingly, cognitive performance in PD has been consistently seen to correlate with GM structural parameters (Garcia-Diaz et al. 2018; Mak et al. 2014), and with functional connectivity (Hugo Cesar Baggio et al. 2015). Baggio and colleagues found that PD-MCI patients had reduced functional connectivity between the dorsal attention network and frontoinsular regions, as well as increased connectivity between posterior cortical regions and the default mode network, which in turn correlated with the attention/executive and visuospatial/visuoperceptual functions (Baggio et al. 2015). Graph theory approaches also showed that PD-MCI had increased clustering coefficient, small-worldness and modularity measures, which were negatively associated with visuospatial/visuoperceptual and memory scores (Baggio et al. 2014). All this taken together suggests that WM might be playing a secondary role in the cognitive impairment of PD. On the other hand, beyond the acceptance of MCI definition (Litvan et al. 2012) as useful clinical criteria to identify patients with worse cognitive profiles and dementia risk, recent evidence suggested the existence of a more complex picture, identifying PD subtypes based on neuropsychological, clinical and MRI data (Dujardin et al. 2013; Fereshtehnejad et al. 2017; Uribe et al. 2016, Inguanzo et al. 2021). In light of our results, it could be suggested that the study of structural connectivity in PD subtypes might facilitate the study of different patterns of cognitive deterioration and shed light on their anatomical basis/substrates. Future studies should consider a whole-brain approach to better describe structural connectivity abnormalities in PD subtypes and its possible association with cognitive impairment. Moreover, combining neuroimaging with clinical data would allow for better precision in finding PD subgroups.

CONCLUSION

In conclusion, whole-brain structural connectivity techniques based on probabilistic tractography allow identification of reduced connectivity in fronto-striatal and posterior cortical connections related to cognitive decline in PD and are able to reveal potential structural connectivity indicators to classify PD disease phenotypes with high accuracy.

ACKNOWLEDGEMENTS

We are grateful to all the participants in the study for their goodwill and generosity. We are also indebted to the Magnetic Resonance Imaging core facility of the IDIBAPS for technical support; and we acknowledge the CERCA Programme/Generalitat de Catalunya.

AUTHOR'S CONTRIBUTION

CJ and BS contributed to the research project conception and in the design of the study. AA, AC and CU contributed to the acquisition of the data. AI, RS, GM contributed to the analysis of the data and AI, BS, RS, GM, AA, AC, CU, HCB, YC, MJM, FV, NB and CJ contributed to the interpretation of the data. AI and BS contributed to the draft of the article. AI, BS, RS, GM, AA, AC, CU, HCB, YC, MJM, FV, NB and CJ revised the manuscript critically for important intellectual content and approved the final version of the manuscript.

DISCLOSURES & FUNDING

This study was sponsored by the Spanish Ministry of Economy and Competitiveness (PSI2013-41393-P; PSI2017-86930-P cofinanced by Agencia Estatal de Investigación (AEI) and the European Regional Development Fund), by Generalitat de Catalunya (2017SGR 748), Fundació La Marató de TV3 in Spain ([20142310](#)), and supported by María de Maeztu Unit of Excellence (Institute of Neurosciences, University of Barcelona) MDM-2017-0729, Ministry of Science, Innovation and Universities. AI and AC were supported by APIF predoctoral fellowship from the University of Barcelona (2017–2018). AA was supported by a fellowship from 2016, Departament d'Empresa i Coneixement de la Generalitat de Catalunya, AGAUR (2016FI_B 00360). CU was supported

by the European Union's Horizon 2020 research and innovation programme under the Marie Skłodowska-Curie fellowship [grant agreement 888692].

MJM received honoraria for advice and lecture from Abbvie, Bial and Merzt Pharma and grants from Michael J. Fox Foundation for Parkinson Disease (MJFF): MJF_PPMI_10_001, PI044024.

YC has received funding in the past five years from FIS/FEDER, H2020 programme, Union Chimique Belge (UCB pharma), Teva, Medtronic, Abbvie, Novartis, Merz, Piramal Imaging, and Esteve, Bial, and Zambon. YC is currently an associate editor for Parkinsonism and Related Disorders.

BIBLIOGRAPHY

- Aarsland D, Brønnick K, Larsen JP, et al. Cognitive Impairment in Incident, Untreated Parkinson Disease: The Norwegian ParkWest Study. *Neurology* 2009; 72(13): 1121–26.
- Abbasi N, S. M. Fereshtehnejad, Y. Zeighami, et al. Predicting Severity and Prognosis in Parkinson's Disease from Brain Microstructure and Connectivity. *Neuroimage Clin* 2020; 25.
- Abos A, Baggio HC, Segura B, et al. Differentiation of Multiple System Atrophy from Parkinson's Disease by Structural Connectivity Derived from Probabilistic Tractography. *Sci Rep* 2019a; 9(1): 1–12.
- Abos A, Segura B, Baggio HC, et al. Disrupted Structural Connectivity of Fronto-Deep Gray Matter Pathways in Progressive Supranuclear Palsy. *Neuroimage Clin* 2019b; 23.
- Agosta F, Canu E, Stefanova E et al. Mild Cognitive Impairment in Parkinson's Disease Is Associated with a Distributed Pattern of Brain White Matter Damage. *Hum Brain Mapp* 2014; 35(5): 1921–29.
- Antonini A, Barone P, Marconi R, et al. The Progression of Non-Motor Symptoms in Parkinson's Disease and Their Contribution to Motor Disability and Quality of Life. *J Neurol* 2012; 259(12): 2621–31.
- Bach M, Laun BF, Leemans A, et al. Methodological considerations on tract-based spatial statistics (TBSS). *Neuroimage* 2014; 100: 358-69.
- Baggio HC, Abos A, Segura B, et al. Statistical Inference in Brain Graphs Using Threshold-Free Network-Based Statistics. *Hum Brain Mapp* 2018; 39(6): 2289–2302.
- Baggio HC, Sala-Llonch R, Segura B, et al. Functional Brain Networks and Cognitive Deficits in Parkinson's Disease. *Hum Brain Mapp* 2014; 35(9): 4620–34.
- Baggio HC, Sala-Llonch R, Segura B. Cognitive Impairment and Resting-State Network Connectivity in Parkinson's Disease. *Hum Brain Mapp* 2015; 36(1): 199–212.

- Barbagallo G, Caligiuri ME, Arabia G, et al. Structural Connectivity Differences in Motor Network between Tremor-Dominant and Nontremor Parkinson's Disease. *Hum Brain Mapp* 2017; 38(9): 4716–29.
- Behrens TEJ, Berg HJ, Jbabdi S, et al. Probabilistic Diffusion Tractography with Multiple Fibre Orientations: What Can We Gain? *Neuroimage* 2007. 34(1): 144–55.
- Dalaker TO, Zivadinov R, Larsen JP, et al. Gray Matter Correlations of Cognition in Incident Parkinson's Disease. *Mov Disord* 2010; 25(5): 629–33.
- Desikan RS, Ségonne F, Fischl B, et al. An Automated Labeling System for Subdividing the Human Cerebral Cortex on MRI Scans into Gyral Based Regions of Interest. *Neuroimage* 2006; 31(3): 968–80.
- Dujardin K, Leentjens AFG, Langlois C, et al. The Spectrum of Cognitive Disorders in Parkinson's Disease: A Data-Driven Approach. *Mov Disord* 2013; 28(2): 183–89.
- Fereshtehnejad SM, Zeighami Y, Dagher A, and Postuma RB. Clinical Criteria for Subtyping Parkinson's Disease: Biomarkers and Longitudinal Progression. *Brain* 2017; 140(7): 1959–76.
- Filipek PA, Christian R, Kennedy DN, and Caviness VS. The Young Adult Human Brain: An MRI-Based Morphometric Analysis. *Cereb Cortex* 1994; 4(4): 344–60.
- Fischl B and Dale A. Measuring the Thickness of the Human Cerebral Cortex from Magnetic Resonance Images.
- Galantucci S, Agosta F, Stefanova E, et al. Structural Brain Connectome and Cognitive Impairment in Parkinson Disease. *Radiology* 2017. 283(2): 515–25.
- Garcia-Diaz AI, Segura B, Baggio HC, et al. Structural Brain Correlations of Visuospatial and Visuo-perceptual Tests in Parkinson's Disease. *J Int Neuropsychological Soc* 2018; 24(1): 33–44.
- Garcia-Garcia D, Clavero P, Gasca-Salas C, et al. Posterior Parietooccipital Hypometabolism May Differentiate Mild Cognitive Impairment from Dementia in Parkinson's Disease. *Eur J Nucl Med Imaging* 2012. 39(11): 1767–77.

- Gou L, Zhang W, Li C, et al. Structural Brain Network Alteration and Its Correlation with Structural Impairments in Patients with Depression in de Novo and Drug-Naïve Parkinson's Disease. *Front Neurol* 2018; 9(JUL): 1–9.
- Griffa A, Baumann PS, Thiran JP, and Hagmann P. Structural Connectomics in Brain Diseases. *Neuroimage* 2013; 80: 515–26.
- Halliday GM, Leverenz JB, Schneider JS, and Adler CH. The Neurobiological Basis of Cognitive Impairment in Parkinson's Disease. *Mov Disord* 2014; 29(5): 634–50.
- Hattori T, Orimo S, Aoki S, et al. Cognitive Status Correlates with White Matter Alteration in Parkinson's Disease. *Hum Brain Mapp* 2012; 33(3): 727–39.
- Inguanzo A, Sala-Llonch R, Segura B, et al. Hierarchical cluster analysis of multimodal imaging data identifies brain atrophy and cognitive patterns of Parkinson's disease. *PARKINSONISM RELAT D* 2021; 82:16-23.
- Jbabdi S, Sotiropoulos SN, Savio AM, et al. Model-Based Analysis of Multishell Diffusion MR Data for Tractography: How to Get over Fitting Problems. *Magn Reson Med* 2012; 68(6): 1846–55.
- Jenkinson M, Bannister P, Brady M, and Smith S. Improved Optimization for the Robust and Accurate Linear Registration and Motion Correction of Brain Images. *Neuroimage* 2002; 17(2): 825–41.
- Jeurissen, B., Leemans, A., Jones, et al. Probabilistic fiber tracking using the residual bootstrap with constrained spherical deconvolution. *Hum. Brain Mapp.* 2011 32: 461–79.
- Kalia, Lorraine V., and Anthony E. Lang. Parkinson's Disease. *Lancet* 2015; 386(9996): 896–912.
- Li, Xiang Rong, Yan De Ren, Bo Cao, and Xuan Li Huang. Analysis of White Matter Characteristics with Tract-Based Spatial Statistics According to Diffusion Tensor Imaging in Early Parkinson's Disease. *Neurosci Lett* 2018; 675: 127–32.

- Litvan I, Goldman GJ, Tröster AI, et al. Diagnostic Criteria for Mild Cognitive Impairment in Parkinson's Disease: Movement Disorder Society Task Force Guidelines. *Mov Disord* 2012; 27(3): 349–56.
- Mak E, Zhou J, Tan LCS, et al. Cognitive Deficits in Mild Parkinson's Disease Are Associated with Distinct Areas of Grey Matter Atrophy. *J Neurol, Neurosurgery and Psychiatry* 2014; 85(5): 576–80.
- Melzer TR, Watts R, MacAskill MR, et al. White Matter Microstructure Deteriorates across Cognitive Stages in Parkinson Disease. *Neurology* 2013; 80(20): 1841–49.
- Mishra VR, Sreenivasan KR, Yang Z, et al. Unique White Matter Structural Connectivity in Early-Stage Drug-Naive Parkinson Disease. *Neurology* 2020; 94(8): 774–84.
- Mori S and Van Zijl PCM. Fiber Tracking: Principles and Strategies - A Technical Review. *NMR Biomed* 2002; 15(7–8): 468–80.
- Muller J, Alizadeh M, Mohamed FB, et al. Clinically Applicable Delineation of the Pallidal Sensorimotor Region in Patients with Advanced Parkinson's Disease: Study of Probabilistic and Deterministic Tractography. *J Neurosurg* 2019; 131(5): 1520–31.
- Nigro S, Ricelli R, Passamonti L, et al. Characterizing Structural Neural Networks in de Novo Parkinson Disease Patients Using Diffusion Tensor Imaging. *Hum Brain Mapp* 2016; 37(12): 4500–4510.
- Peña-Nogales O, Ellmore TM, De Luis-García R, et al. Longitudinal Connectomes as a Candidate Progression Marker for Prodromal Parkinson's Disease. *Front Neurol* 2019; 13(JAN): 1–13.
- Pereira JB, Weintraub D, Brønneck K, et al. Initial Cognitive Decline Is Associated with Cortical Thinning in Early Parkinson Disease. *Neurology* 2014; 82.
- Rubinov M and Sporns O. Complex Network Measures of Brain Connectivity: Uses and Interpretations. *Neuroimage* 2010; 52(3): 1059–69.
- Schapira AHV, Chaudhuri KR and Jenner P. Non-Motor Features of Parkinson Disease. *Nat Rev Neurosci* 2017; 18(7): 435–50.

Segura B, Baggio HC, Marti MJ, et al. Cortical Thinning Associated with Mild Cognitive Impairment in Parkinson's Disease. *Mov Disord* 2014; 29(12): 1495–1503.

Seidman LJ, Faraone SV, Goldstein J, et al. Reduced Subcortical Brain Volumes in Nonpsychotic Siblings of Schizophrenic Patients: A Pilot Magnetic Resonance Imaging Study. *Am J of Med Genet - Neuropsychiatric Genetics* 1997; 74(5): 507–14.

Shah A, Lenka A, Saini J, et al. Altered Brain Wiring in Parkinson's Disease: A Structural Connectome-Based Analysis. *Brain Connect* 2017; 7(6): 347–56.

Smith SM, Jenkinson M, Johansen-Berg H, et al. Tract-Based Spatial Statistics: Voxelwise Analysis of Multi-Subject Diffusion Data. *Neuroimage* 2006; 31(4): 1487–1505.

Tomlinson CL, Stowe R, Patel S, et al. Systematic Review of Levodopa Dose Equivalency Reporting in Parkinson's Disease. *Mov Disord* 2010; 25(15): 2649–53.

Uribe C, Segura B, Baggio HC, et al. Patterns of Cortical Thinning in Nondemented Parkinson's Disease Patients. *Mov Disord* 2016; 31(5): 699–708.

Wang W, Mei M, Gao Y, et al. Changes of Brain Structural Network Connection in Parkinson's Disease Patients with Mild Cognitive Dysfunction: A Study Based on Diffusion Tensor Imaging. *J Neurol* 2019; 267(4): 933–43.

Williams-Gray CH, Foltynie T, Brayne CEG, et al. Evolution of Cognitive Dysfunction in an Incident Parkinson's Disease Cohort. *Brain* 2007; 130(7): 1787–98.

Worker A, Blain C, Jarosz J, et al. Diffusion Tensor Imaging of Parkinson's Disease, Multiple System Atrophy and Progressive Supranuclear Palsy: A Tract-Based Spatial Statistics Study. *PLoS ONE* 2014; 9(11).

Wu L, Liu F, Ge J, et al. Clinical Characteristics of Cognitive Impairment in Patients with Parkinson's Disease and Its Related Pattern in 18F-FDG PET Imaging. *Hum Brain Mapp* 2018; 39(12): 4652–62.

Zalesky A, Fornito A and Bullmore ET. Network-Based Statistic: Identifying Differences in Brain Networks. *Neuroimage* 2012; 53(4): 1197–1207.

Zhang Yu, Burock Marc A. Diffusion Tensor Imaging in Parkinson's Disease and Parkinsonian Syndrome: A Systematic Review. *Front Neurol* 2020; 11: 531993

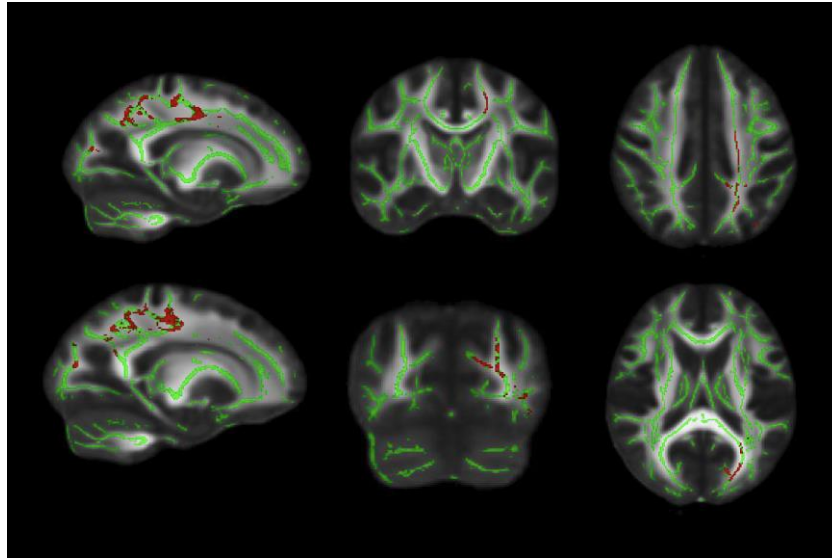


Figure 1. White matter maps (in green) showing regions of significant decreased FA in PD-MCI patients compared with HC (in red). Results were adjusted by gender ($p < 0.05$, FWE-corrected). Radiological convention is used. Abbreviations: FA – Fractional anisotropy; HC - Healthy controls; MCI – Mild Cognitive Impairment; PD – Parkinson’s disease; WM – White matter.

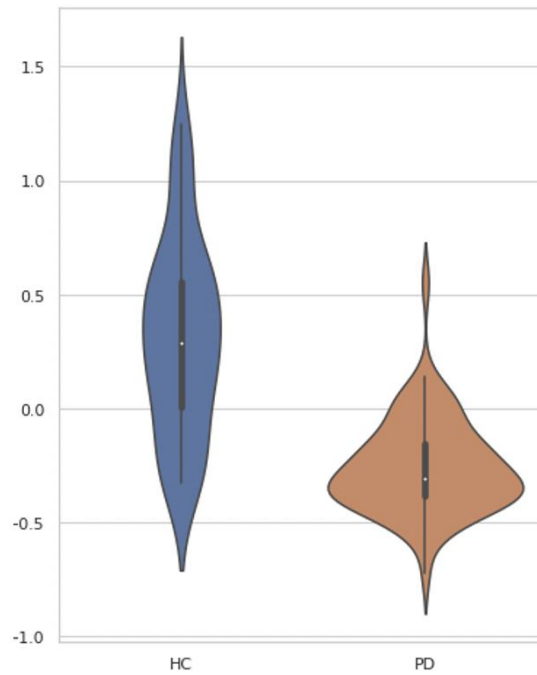


Figure 2. Comparison of mean connectivity between HC and PD patients. Plots illustrate the distribution of average NOS derived from the 114 connections with significantly reduced connectivity in PD compared to HC. Significance of intergroup analyses (FWE-corrected, $p < 0.05$) are shown. Abbreviations: HC – Healthy controls; NOS – Number of streamlines; PD – Parkinson’s disease; TFNBS – Threshold-free network-based statistics.

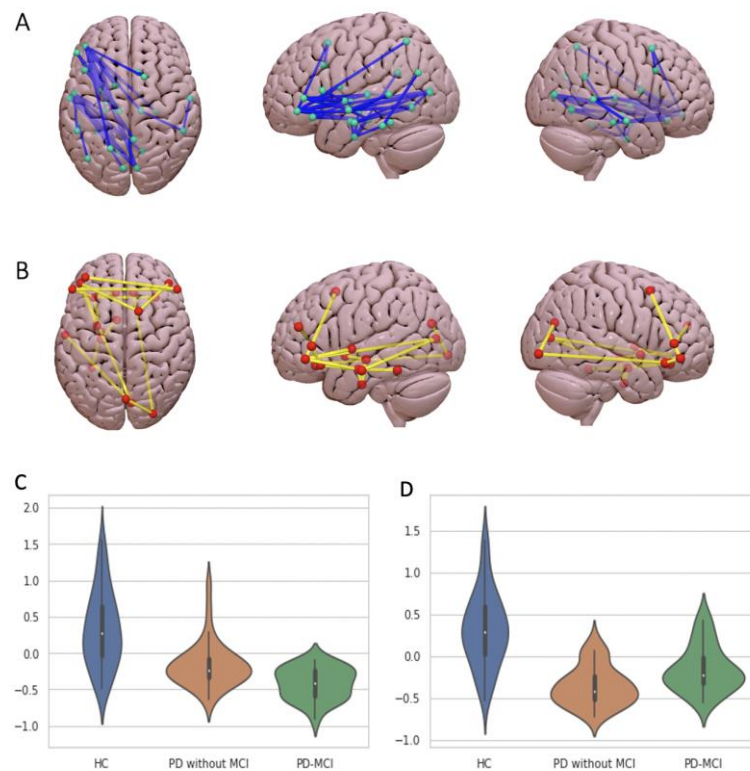


Figure 3. Schematic representation of the structural connections with reduced structural connectivity strength in PD-MCI (A) and PD without MCI (B) compared with HC using TFNBS. Violin plots illustrate the distribution of the measures of average NOS obtained using TFNBS: connections derived from (C) the 37 significantly reduced tracts found in PD-MCI patients compared to HC and (D) the 18 significantly reduced tracts found in PD without MCI compared to HC. NOS values were Z-transformed to allow better comparability. Connectivity figures were drawn using Surf Ice (www.nitrc.org). Significance of intergroup analyses (FWE-corrected, $p < 0.05$) are shown. Neurological convention is used. Abbreviations: HC – Healthy controls; MCI – Mild Cognitive Impairment; PD – Parkinson's disease patients; TFNBS – Threshold-free network-based statistics.

Table 1. Sociodemographic and clinical data. Group differences were assessed using Kruskal-Wallis or Mann-Whitney U test according to the number of groups being compared. Categorical variables were analyzed with Pearson's chi squared test. Abbreviations: HC – healthy controls; IQ – interquartile range; LEDD – L-dopa equivalent daily dose; MCI – mild cognitive impairment; NA – not applicable; PD – Parkinson's disease; UPDRS – Unified Parkinson's Disease Rating Scale

	HC (n=51)	PD without MCI (n=35)	PD-MCI (n=27)	Stats (p-value)
Sex (m/f)	23/28	27/8	19/8	10.26 (0.006)
Age, median(IQ)	66 (17)	63 (11)	68 (16)	2.54 (0.28)
Education, years, median	12(7)	14(10)	11(7)	2.70(0.26)
Disease duration, years, median (IQ)	NA	7 (6.25)	8 (9.25)	537.5 (0.36)
Age of onset, median (IQ)	NA	55.5 (12)	55.5 (21)	477 (0.601)
LEDD, mg, median (IQ)	NA	526.75 (362.5)	575 (502.5)	495 (0.79)
UPDRS part III, median (IQ)	NA	15 (9.75)	15 (10)	446 (0.83)

Hoehn & Yahr, n, 1/2/2.5/3	NA	8/20/0/7	2/11/1/13	8.12 (0.04)
MMSE, median (IQ)	0.096 (1.33)	0.11 (1.43)	-0.85 (2.31)	3.43 (0.18)
IADL, median (IQ)	8 (0)	7(2)	7(3)	22.53 (<0.001)

Table 2. Group comparison of neuropsychological performance. Neuropsychological data presented as z-scores. For the statistical analyses Kruskal-Wallis test and Mann-Whitney U test were used. Abbreviations: BNT – Boston naming test; FRT – Facial recognition test; HC – Healthy controls; JLO – Judgment of line orientation Test; PD – Parkinson’s disease; RAVLT – Rey’s auditory verbal learning test; SDMT – Symbol digits modality test; TMTA- Trail making test part A; TMTB – Trail making test part B; TMTAB – Trail taking test B minus A.

	HC	PD without MCI	PD-MCI	Stats (p-value)	Post-hoc
VFD	0.28 (0.95)	0.08 (0.82)	-0.34 (1.87)	11.53 (0.003)	HC vs PD-MCI
JLO	0.25 (1.08)	0.23 (0.59)	-0.35 (1.84)	9.79 (0.007)	HC vs PD-MCI PD without MCI vs PD-MCI
FRT	0.01(1.18)	-0.08 (1.17)	-0.80 (1.45)	13.9 (0.001)	HC vs PD-MCI
Phonemic fluency	-0.60 (1.41)	-0.05 (1.42)	-0.47 (1.33)	3.83 (0.15)	-
Semantic fluency	-0.37 (1.18)	-0.15 (1.27)	-1.21 (1.27)	20.90 (<0.001)	HC vs PD-MCI PD without MCI vs PD-MCI
RAVLT total	0.11 (1.38)	0.32 (1.31)	-0.80 (2.12)	13.17 (0.001)	HC vs PD-MCI PD without MCI vs PD-MCI
RAVLT recuperation	0.03 (1.13)	0.02 (1.90)	-1.33 (2.36)	20.90 (<0.001)	HC vs PD-MCI PD without MCI vs

					PD-MCI
Forward	-0.40	-0.27 (1.16)	-0.64	1.40 (0.50)	-
digits span	(0.90)		(1.44)		
Backward	-0.17	-0.09 (1.13)	-0.33	2.91 (0.23)	-
digits span	(0.76)		(1.06)		
Stroop Word	-0.23	-0.33 (0.95)	-1.62	26.78 (<0.001)	HC vs PD-MCI
	(1.14)		(1.28)		PD without MCI vs PD-MCI
Stroop Color	0.14	-0.17 (0.65)	-1.40	33.34 (<0.001)	HC vs PD-MCI
	(1.14)		(1.27)		noMCI vs PD-MCI
Stroop Word-Color	-0.07	0.01 (0.93)	-1.07	24.17 (<0.001)	HC vs PD-MCI
	(1.18)		(0.86)		PD without MCI vs PD-MCI
SDMT	-0.08	-0.24 (1.08)	-1.15	24.42 (<0.001)	HC vs PD-MCI
	(1.06)		(1.24)		PD without MCI vs PD-MCI
TMTA	0.20	0.30 (0.91)	1.35	18.94 (<0.001)	HC vs PD-MCI
	(1.17)		(1.92)		PD without MCI vs PD-MCI
TMTB	0.32	0.36 (0.94)	1.98	20.82 (<0.001)	HC vs PD-MCI
	(1.70)		(8.20)		PD without MCI vs PD-MCI
TMTBA	2.18	1.73 (1.21)	2.50	9.55 (0.008)	PD without MCI vs PD-MCI
	(1.80)		(7.33)		

BNT	0.10 (0.90)	-0.07 (0.94)	0.05 (1.37)	2.77 (0.25)	-
------------	----------------	--------------	----------------	-------------	---

Table 3. Global graph measures. Group differences were assessed using Monte Carlo simulations with 5,000 permutations (FWE-corrected, $p < 0.05$). Abbreviations: HC – Healthy controls; MCI – Mild Cognitive Impairment; PD – Parkinson's disease patients.

	HC	PD	stat (F) / p	
Modularity	0.5260 (0.0176)	0.5244 (0.0133)	0.04/ p = 0.9978	
Normalized Clustering coefficient	1.4506 (0.1399)	1.4946 (0.1661)	1.34/ p = 0.5816	
Mean node degree	68.0465 (3.5116)	68.0465 (3.5116)	3.38/ p= 0.1964	
Small worldness	1.2687 (0.1423)	1.3248 (0.1580)	2.22/ p = 0.3608	
Normalized Path length	1.1284 (0.0169)	1.1284 (0.0169)	3.78 / p = 0.1564	
	HC	PD without MCI	PD-MCI	
Modularity	0.5260 (0.0176)	0.5281 (0.0176)	0.5235 (0.0111)	0.96/p=0.7 73
Normalized Clustering coefficient	1.4506 (0.1399)	1.5040 (0.1795)	1.4763 (0.1620)	0.81/ p= 0.833
Mean node degree	68.0465 (3.5116)	66.6744 (4.6977)	66.9070 (4.3721)	1.68/ p= 0.476
Small worldness	1.2687 (0.1423)	1.3397 (0.1602)	1.3130 (0.1650)	1.33 / p = 0.613
Normalized Path length	1.1284	1.123 (0.016)	1.1255	2.16 / p =

(0.0169)	(0.0288)	0.322	37
----------	----------	-------	----

Table 4. Local graph measures. Group differences were assessed using Monte Carlo simulations with 5,000 permutations (FWE-corrected, $p < 0.05$). Abbreviations: HC – Healthy controls; MCI – Mild Cognitive Impairment; NS – Not significant; PD – Parkinson's disease patients.

LOCAL EFFICIENCY	post hoc p -value			significant contrast
	ROI	HC vs PD without MCI	HC vs PD-MCI	
Left Cuneus	NS	0.0418	NS	HC > PD-MCI
Left lateral orbitofrontal	0.0018	0.01	NS	HC > PD without MCI, HC > PD-MCI
Left lingual	NS	0.0186	NS	HC > PD-MCI
Left medial orbitofrontal	0.0486	NS	NS	HC > PD without MCI
Left pars orbitalis	0.0074	0.002	NS	HC > PD without MCI, HC > PD-MCI
Left pars triangularis	0.0108	0.0016	NS	HC > PD without MCI, HC > PD-MCI
Left pericalcarine	NS	0.03	NS	HC > PD-MCI
Left postcentral	NS	0.009	0.014 4	HC > PD-MCI, PD without MCI > PD-MCI
Left rostral anterior cingulate	NS	0.035	NS	HC > PD-MCI
Left superior temporal	NS	0.0146	NS	HC > PD-MCI

Left temporal pole	0.0378	NS	NS	HC > PD without MCI
Right bankssts	NS	0.035	NS	HC > PD-MCI
Right inferior temporal	0.0124	NS	NS	HC > PD without MCI
Right lateral orbitofrontal	0.0134	NS	NS	HC > PD without MCI
Right medial orbitofrontal	0.0302	NS	NS	HC > PD without MCI
Right postcentral	NS	0.0036	NS	HC > PD-MCI
Right superior parietal	NS	0.0334	0.024 4	HC > PD-MCI, PD without MCI > PD-MCI
Right temporal pole	0.0246	NS	NS	HC > PD without MCI
Left Amygdala	0.033	NS	NS	HC > PD without MCI
Left Hippocampus	NS	0.0176	NS	HC > PD-MCI
Left Putamen	0.0496	NS	NS	HC > PD without MCI
Right Accumbens	NS	NS	0.036 6	PD-MCI > PD without MCI
MEAN NODE DEGREE				
Left bankssts	0.0216	NS	0.049	HC > PD without MCI, PD-MCI > PD without MCI

Left cuneus	NS	0.0446	NS	HC > PD-MCI
Left entorhinal	NS	0.0082	NS	HC > PD-MCI
Left frontal pole	NS	0.0144	NS	HC > PD-MCI
Left inferior temporal	0.0162	NS	NS	HC > PD without MCI
Left lateral orbitofrontal	0.0208	0.0338	NS	HC > PD without MCI, HC > PD-MCI
Left lingual	NS	0.0038	0.034	HC > PD-MCI, PD without MCI > PD-MCI
Left pars opercularis	0.0426	NS	NS	HC > PD without MCI
Left pars orbitalis	0.0014	0.0034	NS	HC > PD without MCI, HC > PD-MCI
Left pars triangularis	0.0136	0.0284	NS	HC > PD without MCI, HC > PD-MCI
Left rostral middle frontal	NS	0.0146	NS	HC > PD-MCI
Right frontal pole	NS	0.0406	NS	HC > PD-MCI
Right inferior parietal	NS	0.0412	0.035 6	HC > PD-MCI, PD without MCI > PD-MCI
Right lateral orbitofrontal	0.0022	NS	NS	HC > PD without MCI

Right pars orbitalis	0.0028	NS	NS	HC > PD without MCI
Left Hippocampus	0.0418	0.0014	NS	HC > PD without MCI, HC > PD-MCI
Right Hippocampus	NS	0.0142	NS	HC > PD-MCI
NODAL CLUSTERING COEFFICIENT				
Left bankssts	NS	NS	0.047	PD without MCI > PD- 2 MCI
Left lateral orbitofrontal	0.0012	0.0032	NS	HC > PD without MCI, HC > PD-MCI
Left lingual	NS	0.0162	NS	HC > PD-MCI
Left medial orbitofrontal	0.0122	0.0382	NS	HC > PD without MCI, HC > PD-MCI
Left pars orbitalis	0.026	0.0024	NS	HC > PD without MCI, HC > PD-MCI
Left pars triangularis	0.01	0.0012	NS	HC > PD without MCI, HC > PD-MCI
Left pericalcarine	NS	0.0194	NS	HC > PD-MCI
Left postcentral	NS	0.0076	0.034	HC > PD-MCI, 2 PD without MCI > PD-

				MCI
Left rostral anterior cingulate	NS	0.0464	NS	HC > PD-MCI
Left rostral middle frontal	0.045	NS	NS	HC > PD without MCI
Left superior temporal	NS	0.009	NS	HC > PD-MCI
Left temporal pole	0.0246	NS	NS	HC > PD without MCI
Left transverse temporal	NS	NS	0.033 6	PD without MCI > PD- MCI
Right bankssts	NS	0.0248	0.051 6	HC > PD-MCI
Right inferiortemporal	0.0084	NS	NS	HC > PD without MCI
Right lateralorbitofront al	0.0146	NS	NS	HC > PD without MCI
Right medialorbitofront al	0.0152	NS	NS	HC > PD without MCI
Right postcentral	NS	0.004	NS	HC > PD-MCI
Right superiorparietal	NS	0.0266	0.035 8	HC > PD-MCI, PD without MCI > PD- MCI

Right temporalpole	0.0298	NS	NS	HC > PD without MCI
Left Accumbens	0.0248	NS	NS	HC > PD without MCI
Left Amygdala	0.0328	NS	NS	HC > PD without MCI
Left Hippocampus	NS	0.0164	NS	HC > PD-MCI
Left Putamen	0.0448	NS	NS	HC > PD without MCI
Right Accumbens	0.0124	NS	0.01	HC > PD without MCI, PD-MCI > PD without MCI